Full ^1H and ^{13}C NMR Chemical Shift Assignment of 1-Pyrenyl Substituted Oligosilanes as a Tool To Differentiate between Intramolecular "Through Space" and "Through Bond" Ground State Interactions

J. Gelan,*,† P. Adriaensens,† D. Vanderzande,† D. Declercq,‡ E. Hermans,‡, and F. C. De Schryver*,‡

Contribution from the Institute for Materials Research—Division Chemistry, Limburg University, Universitaire Campus Gebouw D, B-3590 Diepenbeek, Belgium, and Department of Chemistry, Katholieke Universiteit Leuven, Celestijnenlaan 200F, B-3001 Heverlee, Belgium

Received March 7, 1994®

Abstract: A detailed analysis strategy is developed to realize a full proton and carbon NMR chemical shift assignment of a series of substituted 1-pyrenylsilane derivatives mainly based on direct and long-range proton–carbon chemical shift 2D-correlation spectroscopy. The proton and carbon chemical shifts of two dimethylaniline substituted 1-pyrenylsilane derivatives (P2D and P3D) and a pentafluorophenyl substituted 1-pyrenylsilane derivative (P2F) are compared to nonsubstituted 1-pyrenylsilane derivatives of different silane chain lengths (P2, P3, and P6). Accurate ^{13}C shifts of these compounds are shown to be an important tool to study the character of the ground state interactions in these compounds. They are more sensitive than ^1H shifts, and the interpretation is more straightforward since there is no confusion with possible chemical shift anisotropy effects. The analysis leads to the conclusion that changes in local electron density, caused by a donor group as dimethylaniline or by an acceptor group as pentafluorophenyl, are transferred to the pyrene moiety primarily via "through space" electrostatic polarization effects rather than donor–acceptor effects. The observed changes in chemical shift point to the presence of a significant contribution of folded conformations in the ground state for the α,ω-substituted silane derivatives.

Introduction

A series of α,ω-substituted oligosilanes was synthesized to study intramolecular excited state processes. Intramolecular ground state interactions between the two chromophores are evident from comparison of the absorption spectra of the α,ω-substituted oligosilanes with their monosubstituted reference compound and from time resolved fluorescence spectroscopy.[1,17,18] The interactions between the two chromophores can occur "through space" when the conformations of the silane chain allows the two chromophores to be close in space (folded conformation). However, since it is known that a σ-bonded silicon chain has important electron conjugating properties, in particular in the all-trans conformation (stretched conformation),[19] the possibility of a "through bond" interaction between the two chromophores has to be considered. This distinction between through bond and through space interactions is important in the discussion of photoinduced electron transfer in linked donor–acceptor compounds. It has indeed been shown that in rigid and semirigid structures with donor–acceptor substituents with appropriate strength, through bond interaction is an important path for photoinduced electron transfer.[20]

It has been shown that proton NMR is a useful tool to detect a contribution of folded conformations, indicating that intramolecular ground state interactions occur between the pyrene moieties in α,ω-dipyrenyl compounds.[1-3] The main objective of this paper is to show that, as compared to ^1H shifts, accurate ^{13}C shifts can be used as a superior tool to investigate the character of possible ground state interactions in donor–acceptor α,ω-substituted oligosilanes. For this reason a detailed ^{13}C and ^1H shift analysis is performed using a NMR carbon–proton correlation strategy of silylated pyrenes and of donor–acceptor substituted oligosilanes. In this study a detailed ^{13}C and ^1H NMR correlation analysis of silylated pyrenes and of donor–acceptor substituted oligosilanes

† Limburg University.
‡ Katholieke Universiteit Leuven.
® Abstract published in *Advance ACS Abstracts*, July 15, 1994.

(1) Declercq, D.; Delbeke, P.; De Schryver, F. C.; Van Meervelt, L.; Miller, R. D. *J. Am. Chem. Soc.* **1993**, *115*, 5702–5708.
(2) Reynders, P.; Kühnle, W.; Zachariasse, K. A. *J. Phys. Chem.* **1990**, *94*, 4073.
(3) Reynders, P.; Kühnle, W.; Zachariasse, K. A. *J. Am. Chem. Soc.* **1990**, *112*, 3929.
(4) Lock, *Chem. Ber.* **1937**, *70*, 926.
(5) Sakurai, H.; Tominga, K.; Watanabe, T.; Kumada, M. *Tetrahedron Lett.* **1966**, *5*, 5493.
(6) Ishikawa, M.; Kumada, M.; Sakurai, H. *J. Organomet. Chem.* **1970**, *23*, 63.
(7) Martin, G. E.; Zektzer, A. S. In *Two-Dimensional NMR Methods for Establishing Molecular Connectivity*; VCH Publishers, Inc.: Weinheim, Germany; 1988; pp 58–96 (ISBN 0–89573–703-5).
(8) Patt, L. S.; Shoolery, J. N. *J. Magn. Reson.* **1982**, *46*, 535–539.
(9) (a) Atta-ur-Rahman, In *Nuclear Magnetic Resonance*; Springer-Verlag Inc.: New York, 1986; pp 260–271. (b) Horst Friebolin, In *Basic One- and Two-Dimensional NMR Spectroscopy*; VCH Verlagsgesellschaft: Weinheim, Germany, 1991; (ISBN 3–527–28108–8).
(10) Pretsch, P. D.; Clerc, T.; Seibl, J.; Simon, W. In *Spectral data for Structure Determination of Organic Compounds*; Springer-Verlag: Berlin, Heidelberg, 1989; (ISBN 3-540-51202-0).
(11) Kalinowski, H.; Berger, S.; Braun, S. In *Carbon-13 NMR Spectroscopy*; John Wiley & Sons Ltd.: 1988; (ISBN 0-471-91306-5).
(12) Cooper, M. A.; Manatt, L. *J. Am. Chem. Soc.* **1969**, *91*, 6325.
(13) Rodenburg, L.; de Block, R.; Erkekens, C.; Cornelisse, J. *Recl. Trav. Chim. Pays-Bas* **1988**, *107*, 529.
(14) Bovey, F. A. In *Nuclear Magnetic Resonance Spectroscopy*; Academic Press Inc. Ltd.: London, 1988, pp 448–456 (ISBN 0-12-119752-2).
(15) Wehrli, F. W.; Wirthlin, T. In *Interpretation of carbon-13 NMR spectra*; Heyden & Son Ltd.: 1978; p 27 (ISBN 0-85501-207-2).
(16) (a) Heilbronner, E.; Bock, H. In The HMO Model and its application: 1. Basis and Manipulation; John Wiley & Sons Ltd., Verlag Chemie: 1976; pp 156–195. (b) Dehu, C.; Brédas, J.-L. University de Mons-Hainaut, personal communication.
(17) Declercq, D.; De Schryver, F. C.; Miller, R. D. *Chem. Phys. Lett.* **1991**, *186*, 467.
(18) De Schryver, F. C.; Declercq, D.; Depaemelaer, S.; Hermans, E.; Onkelinx, A.; Verhoeven, J. W.; Gelan, J. *J. Photochem. Photobiol. A*, manuscript accepted for publication.
(19) Miller, R. D.; Michl, J. *Chem. Rev.* **1989**, *89*, 1359 and references cited therein.
(20) (a) Verhoeven, J. W. *Pure Appl. Chem.* **1990**, *62*, 1585. (b) Wegewijs, B.; Scherer, T.; Rettschnick, R. P. H.; Verhoeven, J. W. *Chem. Phys.* **1993**, *176*, 349. (c) Paddon-Row, M. N. *Acc. Chem. Res.* **1994**, *27*, 18 and references cited therein.

0002-7863/94/1516-7877$04.50/0

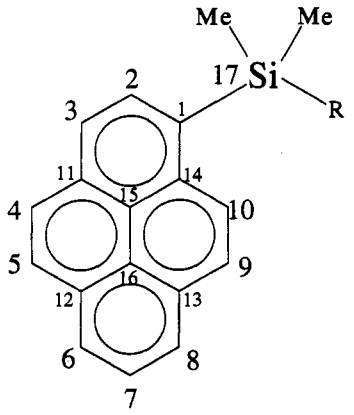

P2 R=Si(Me)$_3$ (18)

P3 R=Si(Me)$_2$Si(Me)$_3$ (18, 19)

P6 R=[Si(Me)$_2$]$_4$-Si(Me)$_3$ (18·21, 22)

P2D R=Si(Me)$_2$-C$_6$H$_3$-N(Me)$_2$ (18, 19, 20, 21, 22, 23)

P3D R=[Si(Me)$_2$]$_2$-C$_6$H$_3$-N(Me)$_2$ (18·19, 20, 21, 22, 23, 24)

P2F R=Si(Me)$_2$-C$_6$F$_3$H$_2$ (18, 19, F20, F21, F22)

Figure 1. Numbering of 1-pyrenyl substituted oligosilanes.

is performed. For the molecules 1-pyrenylpentamethyldisilane (P2), 1-pyrenylheptamethyltrisilane (P3), 1-pyrenyltridecamethylhexasilane (P6), 1-(4-*N*,*N*-dimethylanilino)-2-(1-pyrenyl)-tetramethyldisilane (P2D), 1-(4-*N*,*N*-dimethylanilino)-3-(1-pyrenyl)hexamethyltrisilane (P3D), and 1-(pentafluorophenyl)-2-(1-pyrenyl)tetramethyldisilane (P2F), a full ^{1}H and ^{13}C NMR chemical shift assignment strategy is reported based on two-dimensional proton–proton and carbon–proton correlation spectroscopy. The ^{1}H and ^{13}C shifts, relative to the reference compound P6, are used as probes to evaluate changes in electron density of the pyrene ring for P3, P2, P3D, P2D, and P2F in their ground state. These shift effects are correlated with through space and/or through bond intramolecular interactions.

Experimental Section

a. Syntheses of the Pyrene Derivatives. The syntheses of 1-pyrenylpentamethyldisilane (P2), 1-pyrenylheptamethyltrisilane (P3), and 1-pyrenyltridecamethylhexasilane (P6) are published elsewhere.[1]

1-Pyrenyllithium could be synthesized using 1-bromopyrene[4] and 2 equiv of *tert*-butyllithium.[1] 1,2-Dichlorotetramethyldisilane and 1,3-dichlorohexamethyltrisilane were synthesized using previously reported procedures[5,6] and were distilled over calcium hydride before use. The synthesis of the donor–acceptor substituted oligosilanes involves the substitution of chlorine at one end of the silane chain with 1-pyrenyllithium, followed by the substitution of chlorine at the other end of the chain by the Grignard reagent of *p*-bromo-*N*,*N*-dimethylaniline for P2D and P3D or by the lithium reagent of bromopentafluorobenzene for P2F.

b. NMR Spectra. NMR spectra of perdeuterated cyclohexane solutions are recorded with a VARIAN UNITY 400 system at a temperature of 25 °C. Brown 5 mm NMR tubes have been used in order to prevent photochemical degradation of the compounds in solution. ^{1}H and ^{13}C shifts are calibrated against TMS, while ^{19}F shifts for P2F are calibrated against CF_3COOH at −78.5 ppm. In order to investigate the importance of the intramolecular versus the intermolecular contributions to the shift effects, the carbon and proton spectra were recorded at a higher (±50 mM) as well as at a lower (6.4 mM) concentration. For the P3 molecule systematic ^{1}H and ^{13}C shift measurements were performed in perdeuterated cyclohexane solutions varying in concentration from 10 to 71 mM. For proton NMR standard 1D spectra and 2D-COSY spectra[7] were recorded. For carbon quantitative 1D spectra and attached proton test spectra (APT)[8] were used. Carbon–proton 2D-heteronuclear correlation spectra (HETCOR) were recorded,[9a] using a mixing time corresponding to the direct coupling $^1J_{CH}$ of 140 Hz or a mixing time corresponding to the long range couplings $^2J_{CH}$ or $^3J_{CH}$ of 8 Hz. For sensitivity reasons the HETCOR spectra were recorded using higher concentrations.

In a HETCOR spectrum, the 1D spectra of both nuclei appear on the two axes of the 2D contour plot, and the cross peaks appear in the plot at points corresponding to the chemical shifts of the coupling nuclei. During a well defined mixing period ($\Delta = 1/2J$) magnetization transfer occurs between ^{1}H and ^{13}C nuclei depending on the value of the coupling constant. If a mean value of 140 Hz is used, nuclei of sp^3- or sp^2 hybridized atoms with direct couplings to protons ($^1J_{CH}$) are observed. If the value of J_{CH} is set at 5–10 Hz then the longer range couplings ($^2J_{CH}$ and $^3J_{CH}$) are observed.

Results and Discussion

In the first section a strategy based on ^{1}H and ^{13}C 1D spectra and 2D correlation spectra has been developed to make a full chemical shift assignment possible without the necessity to make any chemical shift supposition. Such an analysis permits to discriminate between carbon (or proton) atoms even if their NMR signals are very close together in the spectra. In a second part the ^{1}H and ^{13}C shift differences of P2, P3, P2D, P3D, and P2F compared to P6 have been interpreted in terms of specific intramolecular structural parameters.

Full ^{1}H and ^{13}C Shift Assignment Strategy. The numbering of the molecules P2, P3, P6, P2D, P3D, and P2F is indicated in Figure 1. From the routine 1D-proton and the 2D-COSY spectra three two-spin systems, corresponding to protons 2-3, 4-5 and 9-10, and one three-spin system corresponding to 6-7-8, are recognized. The COSY spectrum (not shown) indicates which proton signals in the systems are correlated. The accurate chemical shifts of the proton two-spin systems are calculated from the formula of the AB system[9a,b] $\Delta\nu = ((\nu_1 - \nu_4)(\nu_2 - \nu_3))^{1/2}$. For the shift of H7 in the three-spin system 6-7-8 the position of the central peak in the triplet is selected, while for H6 and H8 the central position of the doublets is used.

In the following section a general pathway will be developed using P2 as a representative example for ^{1}H and ^{13}C shift assignment starting with a few straightforward proton assignments. This pathway uses a combination of proton–proton homonuclear correlations (C) from the 2D-COSY spectra, direct carbon–proton $^1J_{CH}$ heteronuclear correlations (D), and long range carbon–proton $^2J_{CH}$ (geminal) or $^3J_{CH}$ (vicinal) heteronuclear correlations (G or V) from the 2D-HETCOR spectra. The direct carbon–proton $^1J_{CH}$ correlations (D) also permit the assignment of the carbon signals to quaternary or nonquaternary carbon atoms.

With the chemical structure of this P2 pyrene derivative in mind a diagram showing all possible correlations can be constructed. In this diagram (Table 1) the symbols C will be used for the COSY homonuclear correlations, while the symbols d, v, and g will be used for the possible direct, vicinal, and geminal hetero correlations, respectively. If these correlations are really found in the spectra, these lower case characters will be converted in bold upper case characters. This correlation diagram will be used to develop the analysis pathway (Scheme 1) for a full proton and carbon shift assignment. In the course of the analysis

Table 1. Carbon-Proton and Proton-Proton Shift Correlations for P2.

	H2	H3	H4	H5	H6	H7	H8	H9	H10	H17	H18
C1	G	V							V	V	
C2	D	g									
C3	g	D	v								
C4		V	D	g							
C5			g	D	V						
C6				v	D	g	V				
C7					g	D	G				
C8					v	g	D	v			
C9							V	D	g		
C10								g	D		
C11	V	g	G	V							
C12			V	G	g	V					
C13						V	g	g	V		
C14	V							V	g		
C15		V	V						V		
C16				v	V		V	V			
C17										D	
C18											D
COSY	C		C		C			C			

Scheme 1. Full Carbon–Proton Shift Assignment Route

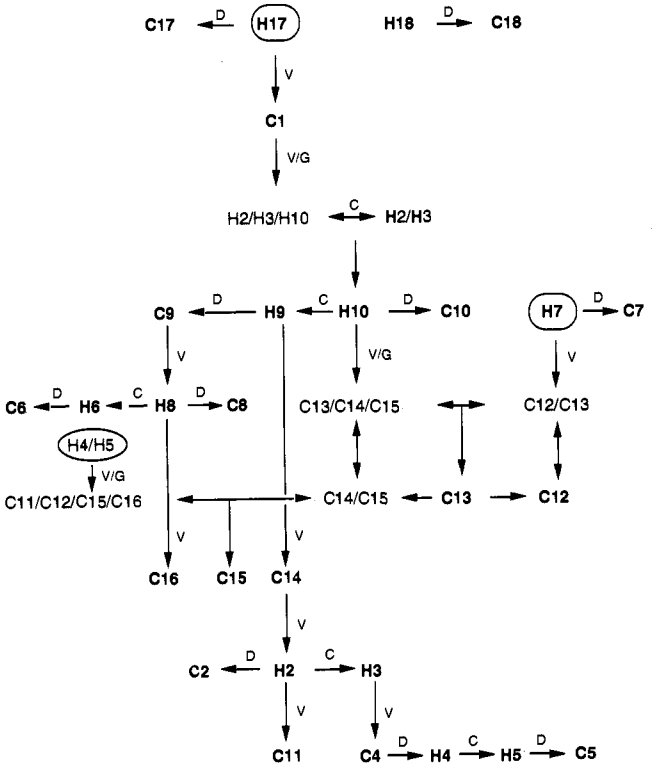

correlations marked with lower case symbols in Table 1 will be converted to uppercase as soon as they are assigned.

In the direct 2D-HETCOR (140 Hz) spectrum (Figure 2) all expected D-interactions are found. Most of the expected V-correlations and some of the G-correlations are present in the long range 2D-HETCOR (8 Hz) spectrum (Figure 3). If in the correlation spectrum no equivocal assignment of G- and V-correlations is possible they will both be considered in the assignment route.

In the development of Scheme 1 the V- and G-correlations are marked as vertical arrows, while for the D- and C-correlations horizontal arrows are used.

The shift of proton 17 is one starting criterion for the full carbon–proton assignment route. From the aliphatic region (not shown) of the routine proton 1D spectrum the relative area of the methyl singlets around 0.18 and 0.62 ppm leads to the assignment of protons 17 and 18, respectively, and also of carbons 17 and 18 through their direct $^1J_{CH}$ correlations. Starting at H17 permits the assignment of C1 through a V-coupling. This C-atom further interacts with the group H2/H3/H10 through remaining G- and V-correlations. In this group H2 and H3 are linked through a C-correlation leaving H10 as assigned. By a D-coupling C10 and by a C-correlation H9 are known leading to C9 by another D-coupling. This C9 further assigns H8 by a V-coupling which assigns C8 by a D-correlation. From H10 more possible V- and G-correlations point to the group C13/C14/C15.

The H7 proton at 7.84 ppm, being the only possible triplet in the proton spectrum, is another starting point in the analysis pathway. It assigns C7 by a D-coupling and permits the assignment of H6 through C-correlations because H8 is already known, while H6 further assigns C6 by a direct D-correlation. The signals of the H4/H5 spin system can now be localized because the other proton spin systems H6/H7/H8, H9/H10, and H2/H3 are situated at this stage. Distinction between H2 and H3, respectively, and between H4 and H5, respectively, will be possible by implementing the long range couplings of the protons with the quaternary C-atoms.

From Table 1 it can be seen that the remaining V-correlations of H7 with the quaternary C-atoms lead to the group C12/C13, while the H4/H5 spin system has remaining possible V- and G-couplings with the group C11/C12/C15/C16. On the other hand, the remaining possible V- and G-correlations of H10 lead to the group C13/C14/C15. A confrontation of the groups C12/C13 and C13/C14/C15 with each other assigns C13 and hence also C12 which localizes then the group C14/C15. A further confrontation of C14/C15 with the group C11/C12/C15/C16 assigns the C15 signal. This also assigns C16 because the correlations of proton H8 with the other C-atoms C6, C7, C8, C9, and C13 are all known by now. The only remaining V-correlation of H9 results in the assignment of C14. From C14 the H2 signal can now be assigned because the possible correlations with H9 and H10 are clarified. H2 leads to C2 by a D- and to H3 by a C-coupling which ends up in C3 by a D-correlation. From H2 the remaining V-coupling leads also to C11, while from H3 the remaining V-coupling brings us to the assignment of C4. A direct coupling of C4 results in the assignment of H4 having a C-coupling to H5 ending up in a D-correlation with C5. A number of V-correlations (C5–H6, C6–H8, C12–H4, C15–H3, and C16–H6) have not even been used in this assignment route but further confirm the analysis which results in a full assignment of the ^1H and ^{13}C chemical shifts of P2.

Because no "a priori" chemical shift suppositions have been made, deviations from the expected shifts, calculated by additivity rules,[10] can now be interpreted as extra arguments for structural analysis and unexpected changes in electron density. For example for C1, being directly linked to a Si-atom, a relatively low (high field) chemical shift could be expected in analogy to the TMS ^{13}C signal at 0 ppm. However, a chemical shift of 136.71 ppm is found instead, suggesting an electron withdrawing effect of silicon when it is linked to a non-sp^3 C-atom.[11] A second example is found in the proton two-spin systems H4–H5 and H9–H10, having higher vicinal coupling constants (±9.1 Hz) compared to the other typical aromatic vicinal coupling constants (±7.6 Hz). This effect points to a higher double bond character for the C4–C5 and C9–C10 bonds in pyrene derivatives[12,13] This vicinal coupling constant is an additional nonbiased extrastructural information since it has not been used in the shift assignments.

The pyrene chemical shift assignments in the other components (P3, P6, P2D, P3D, and P2F) are performed following a similar strategy using an adequate starting criterion depending on the specific molecules. The proton and carbon shifts of all the analyzed molecules are reported in Tables 2 and 3, respectively. For P2D and P3D one starts with the analysis of the *N,N*-

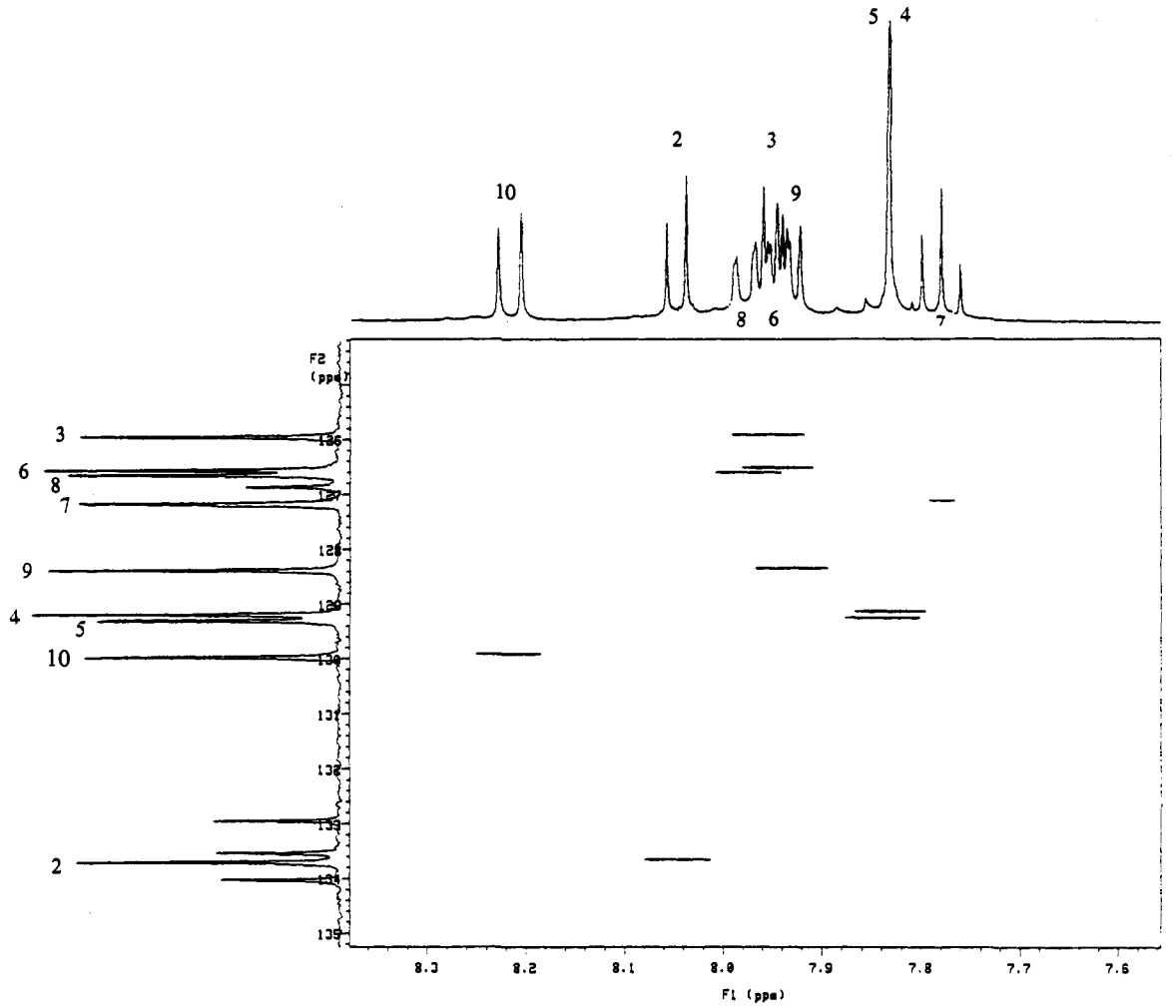

Figure 2. Routine ^{13}C and ^{1}H 1D and direct carbon–proton HETCOR 2D NMR spectrum of P2 using a coupling of 140 Hz as correlation parameter.

dimethylaniline system to assign C17. The methyl protons H24 in P3D, e.g., have a V-correlation with C23 which has another V-coupling with H21, assigning it and thus also H22 by a C-correlation. D-coupling assigns C21 and C22 and a V-coupling of H22 points to C20. This quaternary aniline C-atom linked to Si19 has a V-coupling to H19 while H18 has no proton carbon V-coupling. This brings us to the assignment of H17 which is the same starting point as for the P2-analysis. For P2F the H18 signals in the proton spectrum clearly show a triplet structure due to a long range H–F coupling over five bonds with the ortho substituted F-atoms.[14] Again the remaining H17 will be used as a starting point for the assignment route.

In order to further assign the shifts of the methyl groups in P6, T_1 measurements are performed. The assignment of the methyl protons H17 to H22 is completed based on the expected gradual increased proton mobility in the silanyl side chain when moving away from the connection with the pyrene ring (from H17 to H22).[9] Heterocorrelation between ^{1}H and ^{13}C using a direct $^{1}J_{CH}$ coupling of about 140 Hz results in the assignment of the corresponding carbon atoms C17 to C22.

Interpretation of Shift Differences. The ^{13}C- and ^{1}H-atoms in substituted aromatic systems show marked differences in their chemical shift behavior. Apart from changes in local electron density ^{1}H-shift differences are rather sensitive to through space chemical shift anisotropy effects (CSA) caused by the aromatic π-electron ring currents. The relative importance in ppm of these CSA effects for proton compared to carbon can be understood in view of the rather limited chemical shift range of ±10 ppm for proton compared to ±200 ppm for carbon and by the fact that protons are situated at the outside of the molecules. ^{13}C shifts are more sensitive to local changes in electron density caused by through bond and/or by through space polarization effects than proton shifts. The observed shift effects (in ppm) of ^{13}C are about a factor of 20 more sensitive than ^{1}H as can be observed in Figure 5. Both proton and carbon shifts are sensitive to changes in electron shielding caused by steric hindrance, mostly leading to an upfield shift effect.[15]

In the 1-pyrenyl substituted oligosilanes under investigation the most downfield ^{13}C-shifts for the quaternary aromatic carbons are observed for C1 and C14 (±137.2 and 137.8 ppm) having a higher value of at least 4 ppm compared to the other quaternary C-atoms. For the nonquaternary carbons the most downfield shifts are observed on C2 and C10 (±133.7 and 130.1 ppm) showing a downfield difference of 4 and 1 ppm, respectively. These significant downfield effects on the pyrene C-atoms are observed in the immediate surrounding of the silanyl substituent. This suggests an inductive electron withdrawing effect of the silanyl substituent on the pyrene C-atoms[10] in the vicinity of the Si17–C1 link.

Concentration Effects. An increase in concentration of P3 from 10 to 71 mM causes a small but significant systematic shielding in the ^{1}H spectrum, which is most visible in the region of proton 4 to proton 8 (Figure 4). The largest effect of 0.03 ppm (12 Hz) is observed for proton 5. This upfield chemical shift at higher concentration, which is only about 15% of the effect on the proton shifts in Figure 5, can be explained as an anisotropy effect caused by a weak intermolecular association of the P3 molecules at their sterically less hindered side (4, 5, and 6).

However only a very small (maximum 3 Hz) random carbon shift change has been observed between the ^{13}C NMR of the 10

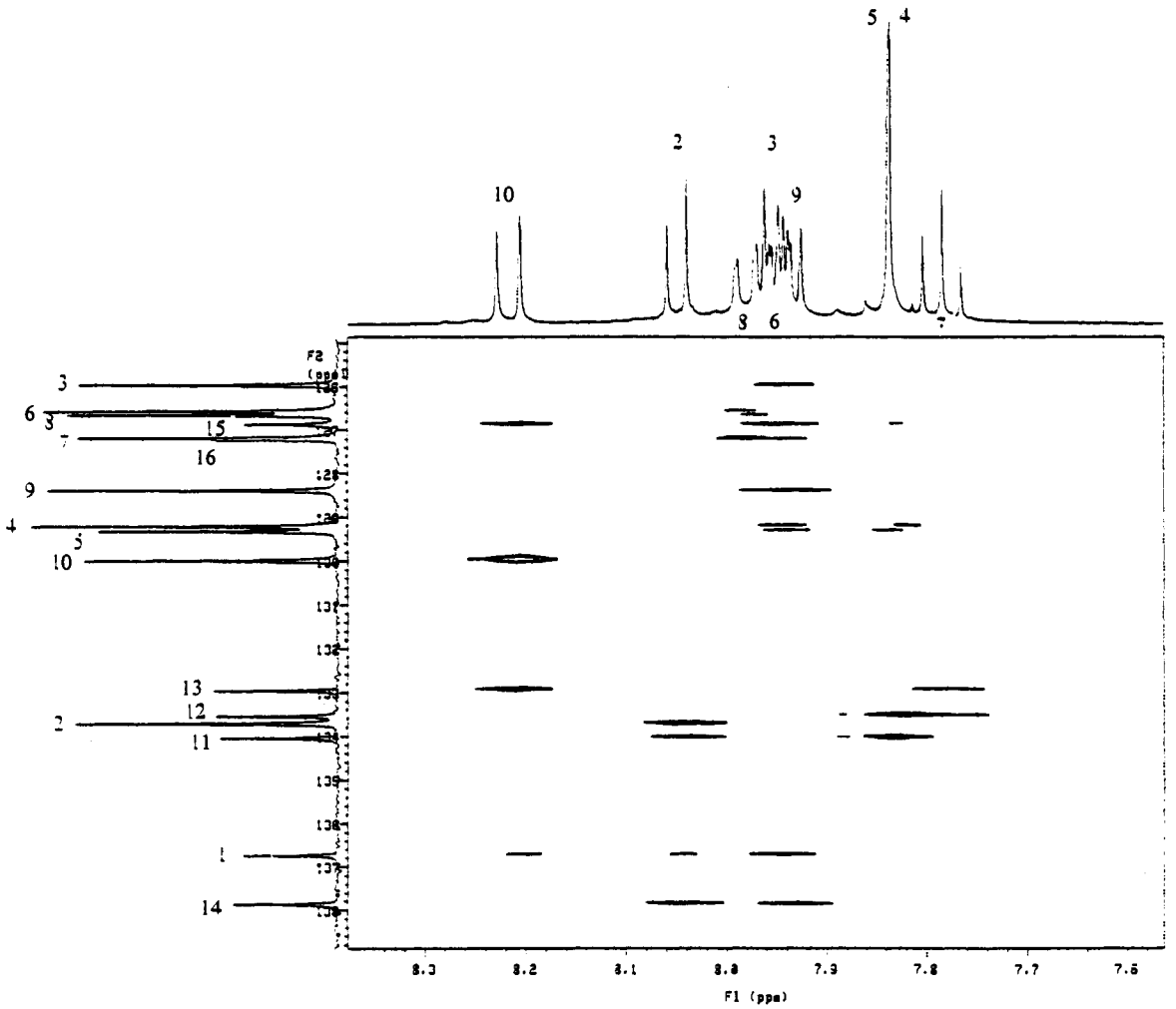

Figure 3. Routine ^{13}C and ^{1}H 1D and long range carbon–proton HETCOR 2D NMR spectrum of P2 using a coupling of 8 Hz as correlation parameter.

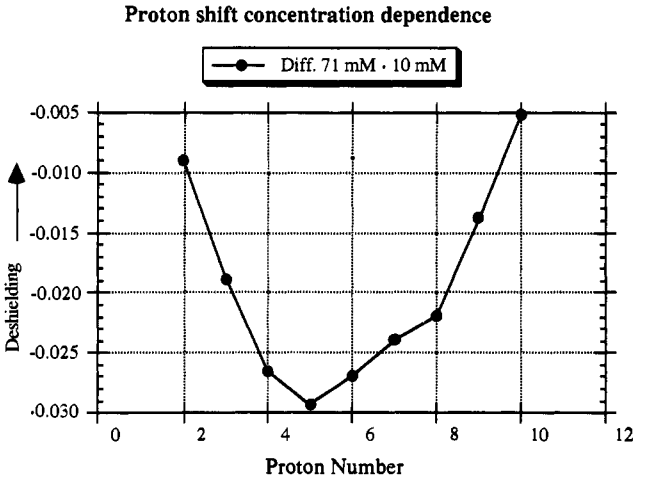

Figure 4. Shift differences of P3 proton spectra when going from 10 to 71 mM concentrations in perdeuterocyclohexane.

mM and the ^{13}C NMR of the 71 mM solution of P3. No significant shift effects could be measured in the ^{13}C spectra of the other molecules in the concentration range from 6.4 to ±50 mM. This indicates that there is no observable intermolecular contribution to the carbon shifts. This confirms that the shifts are an excellent probe to investigate intermolecular electron density effects. In order to avoid significant intermolecular contributions in the interpretation of the proton spectra, a low and constant concentration of 6.4 mM was used for the determination of the proton as well as the carbon shifts of all compounds.

Table 2. Proton Shifts in ppm of P2, P3, P6, P2D, P3D, and P2F Solutions of 6.4 mM in Perdeuterocyclohexane

H-atom	P2	P3	P6[b]	P2D	P3D	P2F
2	8.0754	8.0852	8.0953	8.0603	8.0143	8.0496
3	8.0146	8.0178	8.0187	7.9857	7.9757	8.0214
4	7.9165	7.9171	7.9169	7.9065	7.9110	7.9219
5	7.9325	7.9359	7.9361	7.9185	7.9250	7.9591
6	8.0325	8.0355	8.0360	8.0085	8.0065	8.0605
7	7.8570	7.8590	7.8590	7.8340	7.8380	7.8810
8	8.0520	8.0545	8.0540	8.0085	8.0120	8.0690
9	7.9840	7.9842	7.9852	7.7990	7.8372	7.9424
10	8.2330	8.2538	8.2528	8.0770	8.1128	8.0896
17	0.6215	0.6667	0.6880	0.5711	0.5737	0.6711
18	0.1125	0.1758	0.2603	0.2887	0.2081	0.4424
19	–	–0.0507	0.0121	–	0.1445	–
20	–	–	0.1232	7.1920	–	–45.9[a]
21	–	–	0.0805	6.5520	6.8660	–82.1[a]
22	–	–	0.0518	–	6.1940	–73.1[a]
23	–	–	–	2.8588	–	–
24	–	–	–	–	2.6562	–

[a] ^{19}F shift referenced to CF_3COOH. [b] The ^{1}H T_1 values of H_{17} to H_{22} are 0.83, 0.97, 1.14, 1.24, 1.44, and 1.95 s, respectively.

Silanyl Side-Chain Effects—Proton and Carbon Shift Differences of P2 and P3 Compared to P6. Tables 2 and 3 show that the ^{1}H- and ^{13}C-shifts of the pyrene atoms and of methyl-17 show a levelling off, in going from P2 over P3 to P6. Therefore P6 was chosen as a reference molecule to investigate the shift changes, in agreement with a previous study on di-1-pyrenyl substituted oligosilanes.[1] By using the molecule P6 as a reference, shift

Table 3. Carbon Shifts in ppm of P2, P3, P6, P2D, P3D, and P2F Solutions of 6.4 mM in Perdeuterocyclohexane

C-atom	P2	P3	P6	P2D	P3D	P2F
1	136.79	137.30	137.39	137.29	137.73	134.37
2	133.69	133.71	133.81	133.85	133.77	133.70
3	125.92	125.89	125.90	125.78	125.81	126.01
4	129.20	129.19	129.19	129.18	129.24	129.11
5	129.31	129.34	129.36	129.23	129.12	129.72
6	126.55	126.56	126.59	126.28	126.29	126.95
7	127.17	127.18	127.20	127.01	127.00	127.40
8	126.64	126.66	126.68	126.49	126.55	126.95
9	128.35	128.36	128.37	128.07	128.19	128.71
10	130.00	130.15	130.24	130.48	130.32	129.18
11	134.06	134.05	134.08	133.94	133.92	134.41
12	133.60	133.59	133.60	133.58	133.56	133.50
13	132.99	132.98	132.98	133.03	133.06	132.77
14	137.87	137.89	137.95	137.98	137.94	137.83
15	126.89	126.88	126.91	126.80	126.81	126.77
16	127.25	127.22	127.20	127.21	127.23	127.03
17	–0.64	0.48	0.79	–0.33	0.32	–0.72
18	–0.13	–4.28	–2.59	–1.58	–3.79	–0.55
19	–	–0.19	–2.88	125.72	–1.64	112.44
20	–	–	–2.80	136.73	125.53	150.72
21	–	–	–4.19	114.03	136.20	139.02
22	–	–	0.13	152.66	113.58	143.60
23	–	–	–	41.54	152.13	–
24	–	–	–	–	41.23	–

contributions coming from random conformations of the silanyl side chain are averaged out and accentuating the non-random conformations in the observed shift differences.

Changes in electron density of the pyrene C-atoms around the link with the silanyl side chain depend on the length of this side chain. Compared to P6 only shielding effects are observed for P2 and P3 as well as for the proton as for the carbon shifts. Looking to all the ^{13}C-shifts in Table 3 the most striking upfield shifts of –4.28 and –4.19 ppm are observed for the methyl groups of the silanyl side chain in P3 and P6. These methyl groups are linked to the one but last silicon atom in the silanyl group. This can be understood when we accept that a trisubstituted silyl end group has a significant electron donating effect when it is linked to another Si-atom. This is opposed to the electron withdrawing effect when a silanyl group is linked to a non sp^3 C-atom [10] as in P2, explaining its moderate upfield shift of only –0.64 ppm. The electron donating effect of a trisubstituted silyl end group linked to a Si-atom explains the decreasing shielding effects relative to P6 in the ^{13}C-spectra of Figure 5b when going from C17 over C1 to C10. The same electron donating effect explains the decreasing shielding effects in the ^{1}H-spectra of Figure 5a when going from H17 over H10 to H2. These relative shielding effects are more obvious for P2 as compared to P3 due to the shorter distance of the terminal trisubstituted silyl group in P2. The electron donating through bond inductive effect of the terminal trisubstituted silyl group on the Me-17 groups and on the pyrene ring decreases rather fast as a function of the length of the silanyl side chain. For the carbon and proton atoms at position 10, and maybe also at position 2, a contribution of upfield shift by steric interaction with Me-17 and Me-18 should also be considered.[15]

Proton Shift Differences of P2D, P3D, and P2F Compared to P6. Changes in relative proton shifts compared to P6 as a consequence of the introduction of a dimethylaniline ring or a pentafluorophenyl ring can provide interesting information on the intramolecular interactions causing changes in local pyrene electron densities in the ground state.

Figure 5c shows significant shielding effects for all the proton resonances of P2D and P3D relative to P6. The shielding effects are clearly more pronounced for the protons 9, 10, and 17 in P2D and for the protons 2, 9, 10, and 17 in P3D. Comparable to the dipyrenylsilane compounds[1] the changes on H9 and H10 as well as on H17 can be interpreted as an intramolecular through-space chemical shift anisotropy effect caused by the dimethylaniline ring. This can be explained by a significant fraction of asymmetrically folded conformations in which the dimethylaniline ring is oriented more or less parallel to the pyrene moiety but positioned over the H9-H10 side. Based on space-filling models the effect on H2 and partly the effect on H17, which is also observed in the 1-silanylpyrene model compounds P2 and P3, are believed to originate from changes in steric interactions with Me-17 and Me-18.

Apart from these strong shielding effects a weaker but more overall shielding can be observed on H3 to H8. This overall upfield effect can reasonably well be explained by a rather selective through space polarization effect (vide infra) between the dimethylaniline and the pyrene ring, resulting in a minor overall increased pyrene electron density. A similar but more important effect will be discussed in the analysis of the corresponding ^{13}C-shift differences.

Figure 5e shows the experimental proton chemical shift differences for P2F compared to P6. For the more important shielding effects on H2, H9, and H10 similar conclusions can be drawn as for P2D and P3D. As far as the more overall shift differences for H5 to H8 concern they will again be explained by a through space polarization effect between the pentafluorophenyl and the pyrene ring. This time however a minor decrease in the pyrene electron density is observed.

Carbon Shift Differences of P2D, P3D, and P2F Compared to P6. In the ^{13}C-spectra of the dimethylaniline derivatives the most significant relative shift change in the pyrene ring is the deshielding effect on C1 for P3D and on C10 for P2D (Figure 5d). Significant shielding effects are observed on the atoms C5 to C9 and C11. In the silanyl side chain a clear shielding effect is observed on the C-17 shift, more significant for P2D than for P3D.

All the ^{13}C chemical shift changes of the pyrene moiety in the pentafluorophenyl derivative are opposite relative to P2D and P3D, while the shift change of C1 and C10 is strongly increased. Indeed C1 and C10 show a very strong shielding effect in P2F (Figure 5f), while the atoms C5 to C9 and C11 show a significant deshielding effect. For C-17 of the silanyl side chain however a significant shielding effect similar to P2D is observed.

Fully comparable to the shielding effects of the silanyl side chain in P2 and P3, the shielding effects on C-17, more pronounced in P2D and P2F than in P3D, can be explained by the electron donating effect of a trisubstituted-silyl group linked to a Si-atom. The magnitude and rather fast decrease of the relative shielding as a function of the length of this silanyl side chain demonstrate the limited electrostatic transfer efficiency through the Si–Si backbone. The limitation of this through bond interaction is further demonstrated by the fact that in P3D, P2D, and P2F the atoms C1 and C10 undergo a shift effect opposed to what is expected. For P3D and P2D a deshielding is observed instead of the expected shielding effect of the electron donating dimethylaniline group. For P2F a strong shielding is seen instead of the expected deshielding effect of the electron withdrawing pentafluorophenyl group. The relative shielding effects on C1 and C10 in P2F are even increased compared to P2.

For the P3D and P2D molecules the nonexpected deshielding effects on C1 and C10, respectively, and the shielding effects on C5 to C9 and C11 cannot be explained by chemical shift anisotropy nor by steric interactions. They can however be understood by a through space polarization from the dimethylaniline ring folding over the pyrene moiety. Another mechanism one can envisage is a charge transfer type molecular orbital interaction of the frontier orbitals (HOMO or LUMO) of the pyrene π-system and those (LUMO or HOMO, respectively) of the substituent π-system. In this case one would expect that the nodal properties of the frontier orbitals of pyrene (nodal plain through C2, C15, C16, and C7) should show up as small chemical shift differences only. Despite the symmetry breaking effect of substitution at C1

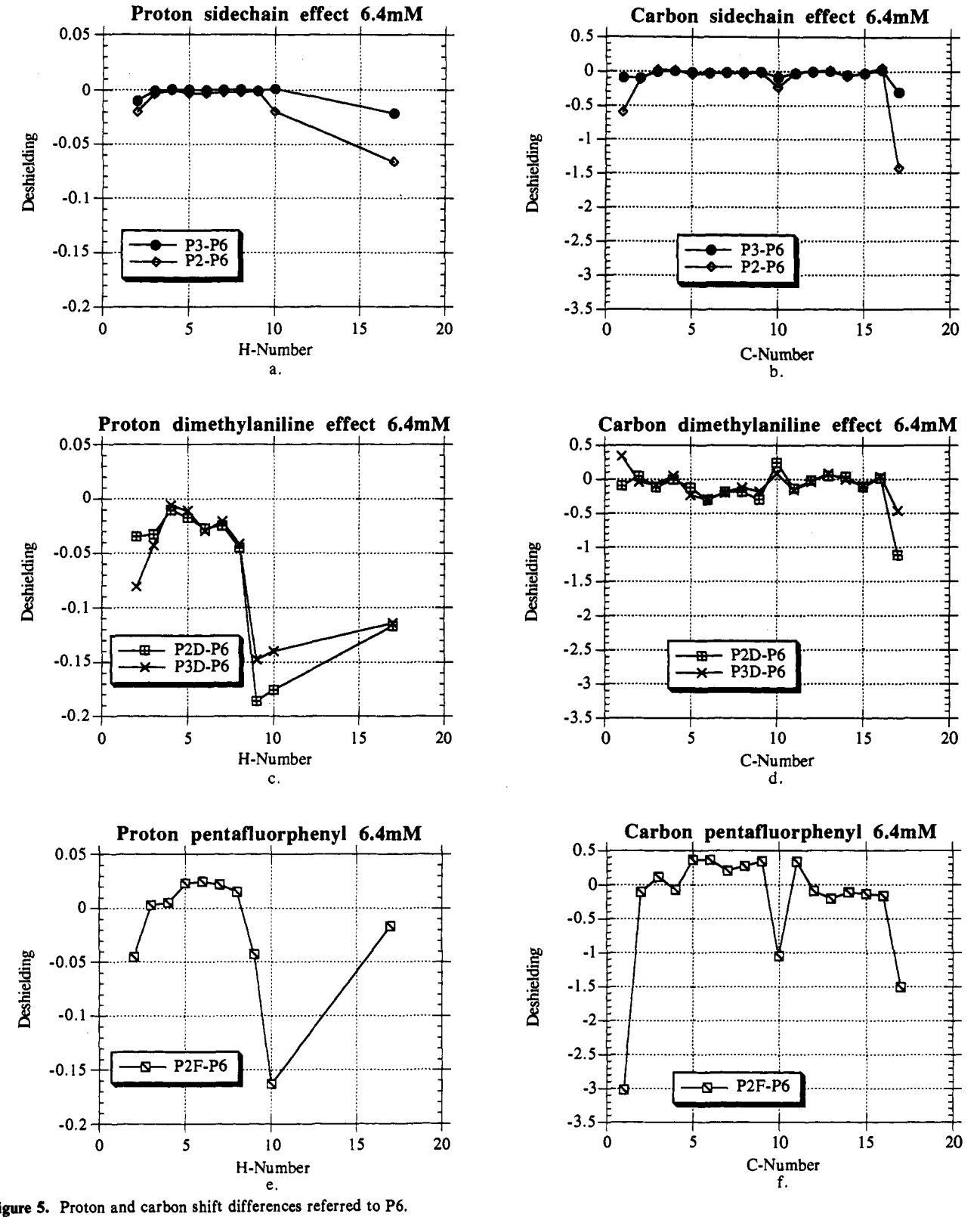

Figure 5. Proton and carbon shift differences referred to P6.

this nodal plane effect is still expected.[16] Such a nodal plane property is however not observed in the ^{13}C chemical shifts. The effects on C7, C15, and C16 are in several cases of comparable magnitude to those on the other carbon atoms.

Molecular models however show that local regions of high and low electron density in the dimethylaniline ring correspond reasonably well with regions of opposed local electron density in the pyrene ring. Based on the expected delocalization effects and on the observed ^{13}C chemical shifts of the *N,N*-dimethylaniline ring, confirmed by additivity rules,[11] a significant increased electron density can be proposed on the ortho C-atoms (–16.1 ppm for C21/C22 in P2D/P3D compared to the normal aromatic shift value of 128.5 ppm). A decreased electron density can be expected on the Me-groups linked to nitrogen, on the quaternary C-atom linked to N (+22.8 ppm for C22/C23), and on the meta C-atoms (+6.8 ppm for C20/C21).[11] For the calculations of these ^{13}C chemical shifts, a trimethyl silyl group is taken for the para-substituent on the quaternary C-atom (C19/C20 in P2D/P3D).

A significant fraction of properly folded conformations, having

atoms in the dimethylaniline ring with increased electron density in the neighborhood of C1 and C10, can induce opposite electron densities in these pyrene ring positions by local through space electrostatic polarization effects. On the other hand, the low electron densities on the atoms C22/C23 and C23/C24, linked to N in P2D/P3D, are responsible for the shielding effects on the pyrene atoms C5 to C9 and C11.

In the pentafluorophenyl substituted derivative P2F (Figure 5f), the change from shielding to deshielding effects on the atoms C5 to C9 and C11 and the reversal of the effects on C1 and C10 in going from P2D and P3D to P2F can again be explained by local through space electrostatic polarization effects. They result from a significant fraction of conformations having the pentafluorophenyl ring folded over the pyrene ring, in agreement with the results of the proton spectra.

Based on the observed ^{19}F and ^{13}C chemical shifts of the pentafluorophenyl ring, confirmed by ^{13}C chemical shift prediction rules[11] (taking again a trimethylsilyl substituent in the C19 position), places of high and low electron density can be estimated in the pentafluorophenyl ring. Compared to the normal value of 128.5 ppm an increasing carbon electron deficiency is expected when going from the meta (+5 ppm for C21) over the para (+15 ppm for C22) to the ortho (+26 ppm for C20) aromatic carbon-atoms. A high electron density is expected for the C19 atom (−16 ppm) and in an increasing order for the F-atoms F20, F22, and F21. In the proposed folded conformations of P2F the ortho C-atoms C20, having the lowest electron density, are positioned in the vicinity of C1 and C10, increasing the shielding by a through space electrostatic interaction. This accentuates the shielding effect which was already induced by the electron donating through bond effect of the trisubstituted silyl end group of the side chain. The F-atoms with their high electron density however cause low electron densities on the atoms C5 to C9 and C11 by the same electrostatic through space interactions. They also result in regions of low electron density on the Me-17 protons.

Conclusion

Using an analysis strategy based on homo- and heteronuclear NMR 2D-correlation spectroscopy an accurate full ^{1}H and ^{13}C chemical shift assignment of a series of substituted 1-pyrenylsilane derivatives could be accomplished. Because no "a priory" chemical shift suppositions had to be made, deviations from the expected shifts can be used as tools to analyze changes in the ground state conformations and electron densities. From the shift analysis of the nonsubstituted 1-pyrenylsilanes as a function of the silane chain length, only a short distance through bond efficiency for electron density transfer is observed in the silane backbone. For the substituted 1-pyrenylsilanes nor electron donor through bond effects from the dimethylaniline ring nor electron withdrawing through bond effects from the pentafluorophenyl ring are noticed on the pyrene shifts. Several through space shift effects however show evidence for an amount of folded conformations in the ground state of the α,ω-substituted silane derivatives. Significant through space electrostatic polarization effects are observed in the ^{13}C NMR spectra, confirming the through space chemical shift anisotropy effects, and the moderate electrostatic polarization effects are observed in the ^{1}H NMR spectra. Through space interactions are important in intramolecular photoinduced electron transfer process in these flexible donor–acceptor substituted silane chains. The presently applied ^{1}H and ^{13}C NMR methodology could be an efficient tool to investigate and to evaluate possible, competitive ground state through bond and/or through space interactions in other linked donor–acceptor systems.

Acknowledgment. The financial support through the Interuniversity Attraction Poles IUAP II-016 and IUAP III-040 initiated by the Belgian State (Prime Minister's Office) Science Policy Programming is gratefully acknowledged. D. D. thanks the N.F.W.O. and the K. U. Leuven for a predoctoral and a postdoctoral fellowship, respectively. E. H. thanks the IWONL for a predoctoral fellowship. The authors also thank Prof. Hadziiannou for helping with the synthesis of P2F and Dr. Miller for assisting with the synthesis of the other oligosilanes.